Interfacial Breakdown between Dielectric Surfaces Determined by Gas Discharge

Emre Kantar, Frank Mauseth, and Erling Ildstad
Department of Electric Power Engineering
Norwegian University of Science and Technology
Trondheim, Norway

Sverre Hvidsten
Electric Power Technology
SINTEF Energy Research
Trondheim, Norway

***Abstract*—This paper examines the influence of the elastic modulus and applied contact pressure on the tangential AC breakdown strength (BDS) of polymer solid-solid interfaces theoretically and experimentally. In the experiments, three different materials with different elastic moduli, namely cross-linked polyethylene (XLPE), cured end product of epoxy resin (EPOXY), and polyether ether ketone (PEEK) were employed under various contact pressures. The BDS of each interface increased as the contact pressure was augmented. As the contact pressure became threefold, the interfacial BDS rose by a factor of 2.4, 1.7, and 1.8 in the case of the PEEK, EPOXY, and XLPE interface in a sequence following the decrease of the elastic modulus. Under the same contact pressure, it was observed that the lower the elastic modulus, the higher the BDS. The proposed theoretical approach tested two different mechanisms in determining the gas pressure inside the cavities. Both mechanisms suggested decreasing BDS values as the elastic modulus was augmented; however, the estimated results deviated widely from the experimental data as the pressure was significantly increased in the case of first proposed mechanism whereas the second mechanism correlated with the experimental data much better.**

***Index Terms*—Cavity, dielectric breakdown, epoxy, gas discharge, partial discharge, PEEK, polymer interface, solid-solid, surface breakdown, void, XLPE.**

I. INTRODUCTION

Cable connectors and joints allow swift, reliable and in situ connection of units to main modules as well as provide adaptability and modularity. They are, thus, inalienable components of the power transmission system. Driving force to provide more energy mandates significant and cost-effective developments in cables and accessories, necessitating higher voltages, temperatures and longer step-out lengths, where total system design is limited by the availability of suitable cable connectors and accessories [1], [2].

Existence of solid-solid interfaces between polymers causes many problems since the dielectric strength of an interface is weaker than that of a bulk insulation due to the presence of microscopic imperfections such as cavities (see Fig. 1), protrusions, and impurities. Such defects reduce the tangential AC electric breakdown strength (BDS) of the interface notably [1], [2]. Even in cases when the magnitude of the tangential electric field is much lower than the dielectric strength of the bulk insulation, the imperfections at the interface cause local electric field enhancements [3]. They are, thus, likely to initiate partial discharges (PD), electrical treeing, and a complete flashover might eventually follow [1]–[3].

The authors acknowledge the financial support of the Research Council of Norway (project no. 228344) and the SUBCONN Project Consortium.

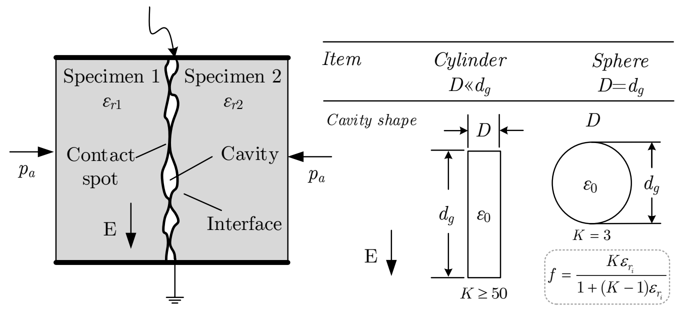

Fig. 1. An illustration of the air-filled cavities (ϵ_0 therein) at the interface in two-dimensional profile. $K \geq 50$ for cylinder, $K = 3$ for sphere.

Elastomers and polymers as insulating materials and BDS thereof have been studied to a large extent in the literature. The interfacial breakdown between two dielectric surfaces was reported to represent one of the principal causes of failure for power cable joints and connectors, in which surface roughness, applied contact pressure, and elastic modulus of the dielectric material play a key role [4], [5]. There is; however, still a lack of knowledge on the theoretical correlation between the elastic modulus and the BDS of the interfacial surfaces. Therefore, the primary objective of this paper is to theoretically and experimentally examine the influence of the elastic modulus on the tangential AC breakdown strength of dry-assembled solid-solid interfaces under various contact pressures.

II. INTERFACIAL CONTACT THEORY

A. Total Area of Contact and Air-filled Cavities

Contact theory in [1] is employed to characterize a dry contact between solid-solid polymers. The contact theory holds the contact spots (i.e. the total real area of contact) and the air-filled microscopic cavities (see Fig. 1) responsible in dominating the interfacial breakdown phenomenon [1]. Ratio of the total real area of contact A_{re} (microscopic) to the nominal contact area A_a (macroscopic) is given by:

$$A_{re}/A_a \simeq 3.2\frac{p_a}{E'\sqrt{\sigma/\beta_m}}, \tag{1}$$

in terms of the applied contact pressure p_a, the effective elastic modulus E' of two materials in contact, the standard deviation of the asperities' heights σ and the mean radius of the asperities' summit β_m [5]. Equation (1) provides a first-hand relation when scrutinizing A_{re} in connection with the interfacial BDS under various E' and p_a.

The breakdown of the air-filled microscopic channels presumably prevail over the breakdown of the contact spots in governing the interfacial BDS; however, either can equally be dominant in some cases, which are mentioned in Section IV.

A flashover across a single cavity or multiple cavities might eventually evolve to interfacial breakdown. However, whether a single or a few large cavities can achieve a complete flashover along the interface was not studied. Nor was the duration until the PD activity evolves to a complete flashover examined. With this limited information, we roughly assume that breakdown of a single cavity is analogous to onset of the PD activity at the interface [2], the PD inception field strength (PDIE) is thus linearly proportional to the interfacial BDS:

$$BDS = \alpha \cdot PDIE, \tag{2}$$

where α is a numerical coefficient.

B. Average Cavity Size

Following the approach in [1], flashover/breakdown voltage of a cavity can be estimated by using the Paschen's curve for air (see Fig. 2) on condition that average cavity size is known, and the applied electric field is homogeneous. The average size of the cavities can be determined by the following assumptions with regards to the contact theory [5]:

- The summits of the asperities are assumed spherical with a mean radius β_m.
- The asperities have a Gaussian distribution in height about a mean plane in a two-dimensional plane.
- The number of air-filled channels is assumed equal to the number of contact spots at the interface, resulting in one contact spot between two consecutive cavities.

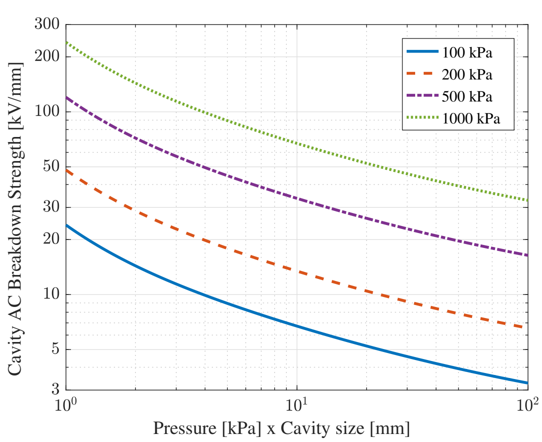

Fig. 2. Left side of the Paschen's curve for air under various air pressure.

After manipulating the set of formulas provided in [1], the correlation between the contact pressure, elastic modulus and the average cavity size d_g is reduced to

$$d_g = \frac{2\left(E'\sqrt{\dfrac{\sigma}{\beta_m}} - 3.2p_a\right)^{0.5} \beta_m^{\,0.47}\,\sigma^{\,0.41}}{\sqrt{1.21\pi}\,E'^{\,0.06}\,\eta^{0.06}\,p_a^{0.44}}, \tag{3}$$

where η is the surface density of asperities [1].

In this paper, only cylindrical cavities elongated in the tangential direction, as depicted in Fig. 1, will be studied because the surface inspection performed in [3] revealed the dominance of such elongated cavities, where the electric field strength inside such cavities is almost equal to that of in the bulk insulation (unity enhancement factor i.e. $f \simeq 1$).

C. Gas Pressure Inside the Air-filled Cavities

1) Mechanism I: As the curves in Fig. 2 delineates, the BDS of a cavity differs as a function the gas pressure confined in the cavity. In the authors' previous work [2], large channels are assumed to be predominating the interfacial BDS. Large channels are presumably formed by a few strings of large cavities, that are vented to their surroundings, hence the pressure inside the cavities (p_c) remains at the ambient pressure i.e. $p_c \simeq 1\,\mathrm{bar}$ irrespective of the applied contact pressure. The validity of this assumption will be tested in the results section.

2) Mechanism II: The contact theory suggests that in the event of elastic contacts, large cavities shrink substantially depending on the elasticity and applied contact pressure. As a result, plenty of solitary interlocked cavities emerge, that are likely to prevail the interfacial breakdown phenomenon [3], [4]. Air pressure inside the enclosed cavities prior to the application of contact pressure p_0 is assumed $1\,\mathrm{bar}$. On the other hand, with the increase of the applied pressure, cavities is further compressed, and hence the pressure inside an average cavity p_c rises according to the ideal gas law:

$$p_c = \left(\frac{d_{g_{ref}}}{d_g}\right)^3 p_0 \tag{4}$$

where $d_{g_{ref}}$ is the initial cavity size in the tangential direction when p_a is equal to the reference initial applied pressure p_{ref}. Subsequently, the Paschen's law is referred to determine the BDS of the cavity at the obtained p_c. The curves in Fig. 2 are plotted by means of the empirically obtained polynomial fit:

$$E_{BD} = A\frac{p_0/p_c}{{d_g}^2} + B(p_c/p_0) + \frac{C}{d_g} + D\sqrt{\frac{p_c/p_0}{d_g}} \tag{5}$$

where $p_0 = 1\,\mathrm{bar}$, A $= 0.00101\,\mathrm{kV}\cdot\mathrm{mm}$, B $= 2.4\,\mathrm{kV/mm}$, C $= -0.0097\,\mathrm{kV}$, D $= 2.244\,\mathrm{kV}\cdot\mathrm{mm}^{-0.5}$ [6].

III. Experimental Procedure

A. Set-up for AC Breakdown Tests

A simple illustration of the test arrangement with the dimensions of the core components is depicted in Fig. 3. There, two rectangular prism-shaped samples (55 mm x 25 mm x 4 mm) were assembled under dry ambient conditions between two Rogowski-type electrodes, forming a 4 mm-wide interface traversed by the tangentially applied field [2]. An AC ramp voltage with the rate of 1 kV/s was applied. Due to limited space, readers are advised to refer to [2], [3], [7] for the details of the test setup and the experimental procedure.

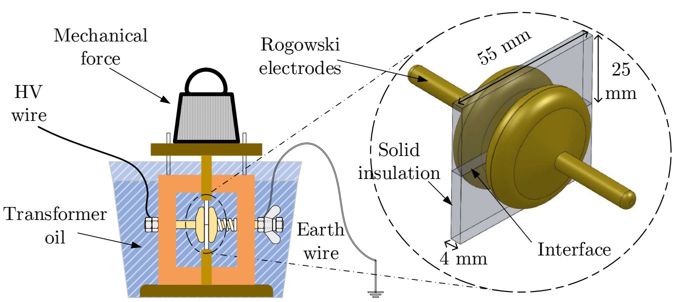

Fig. 3. The simplified sketch of the mechanical test set-up. Electrode diameter 36 mm.

In the experiments, XLPE, EPOXY and PEEK samples were employed to form interfaces between identical materials. The XLPE and PEEK samples were cut in the aforementioned size from a commercial, XLPE-insulated 145 kV power cable and VESTAKEEP 4000R smooth rod [3], respectively. In addition, we cast the epoxy in the laboratory from Casting Resin XB 5950, and Hardener XB 5951 APG [3].

B. Surface Characterization

Bruker Contour GT − K 3D optical profilometer was used to obtain the surface topography of the polished sample surfaces. The assessment area of the profile was about 5.5% of the nominal contact area A_a (4 mm x 55 mm). Several scans were performed at different sections to ensure consistency. Surface characterization parameters of σ, β_m, and η were then obtained following the procedure in [1] and are the summarized in Table I.

TABLE I
SURFACE CHARACTERIZATION PARAMETERS

Interface	σ [μm]	β_m [μm]	η [μm]
XLPE	2.55	6.39	$2.8 \cdot 10^{15}$
EPOXY	3.51	3.45	$2.7 \cdot 10^{15}$
PEEK	2.99	1.38	$7.3 \cdot 10^{15}$

C. Test Procedure and Data Processing

The desired contact pressure was exerted using weights ranging between 25 − 75 kg to press the samples against one another vertically. The average contact pressure is then calculated using $p_a = F/A_a$, where F is the exerted force in N and A_a is the interface area in m^2 (4 mm x 55 mm). Thus, p_a was varied between 11.6 − 33.4 bar. The value of p_{ref} was fixed to 11.6 bar when calculating $d_{g_{ref}}$ in (4). In addition, measured effective elastic moduli E' of the interfaces for XLPE-XLPE, EPOXY-EPOXY, and PEEK-PEEK are: 226, 5166 and 8808, respectively [3]. For each set of experiments, 8 measurements were performed using a virgin pair of samples only once. The obtained results were statistically evaluated each using the two-parameter Weibull distribution.

IV. RESULTS & DISCUSSION

Experimental results published in [3] are directly employed in this paper since the main motivation here is to test the validity of the postulated interface breakdown mechanisms in Section II-C. To summarize, the experimental data presented in Fig. 4 demonstrate that an increased elastic modulus (i.e. a harder material) results in a reduced BDS. The errorbars represent the 90% confidence intervals while the markers stand for the 63.2 percentile. From 11.6 bar to 33.4 bar, the interfacial BDS increased by a factor of 1.8−2.4 following the decrease of the elastic modulus among the chosen materials. Furthermore, the higher the elastic modulus, the wider the confidence intervals as seen in Fig. 4, indicating that harder polymer texture renders the interfacial BDS values comparable particularly when the applied pressure is of low/moderate magnitude.

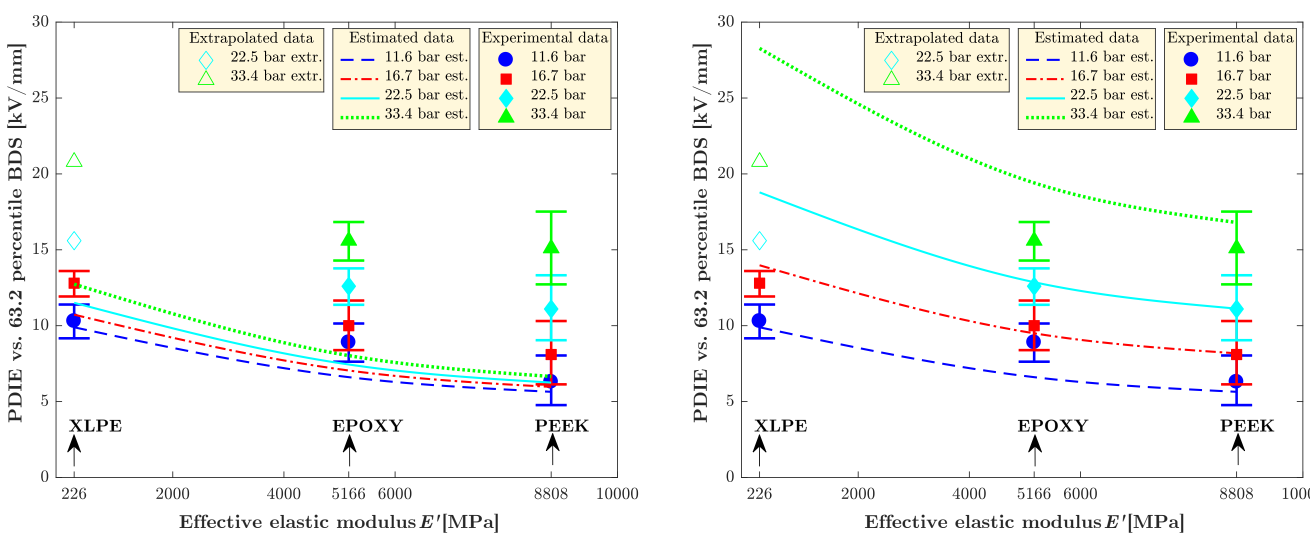

Fig. 4. The 63.2 percentile BDS as a function of the effective elastic modulus: (a) Mechanism I − $p_c = 1$ bar in the voids. (b) Mechanism II − $p_c \propto {d_g}^{1/3}$.

The filled markers in Fig. 4 represent the experimentally obtained values while the hollow markers stand for the extrapolated data (i.e. $\mathrm{extr.}$) extracted from [3]. The necessity for extrapolation was because pressures beyond $16.7\,\mathrm{bar}$ were infeasible due to deformation of the XLPE samples. For a wholesome overview, extrapolated data serve as reference and ease interpretation.

In addition, the estimated BDS values of the cavities (i.e. PDIE) were plotted in Fig. 4 (shown with $\mathrm{est.}$) by means of average cavity sizes obtained using (3) and the tabulated data in Table I for each mechanism mentioned in Section II-C. Resulting α in (2) can then be computed by comparing the estimated PDIE with the experimental $63.2\,\mathrm{percentile}$ BDS.

Speaking of Fig. 4(a), we observed a significant discrepancy between the experimental BDS and the estimated PDIE as the pressure is increased. Thus, much higher α coefficients arise as the pressure is raised. For instance, α varies from 1.1 to 1.6 at 11.6 bar; whereas, the range at 33.4 bar becomes $1.7-2.5$ from XLPE to PEEK. It can, then, be argued that the interfacial breakdown phenomenon is not directly governed by the vented air-filled cavities especially at high contact pressures; in other words, mechanism I starts not to remain valid as the pressure is increased.

In the case of Fig. 4(b), α ranges from 1.04 to 1.11 at 11.6 bar; whereas, it spans $0.77-0.93$ at 33.4 bar as modulus is increased (from XLPE to PEEK). When the confidence intervals are considered, it is somewhat surprising that the PDIE values fit the experimental data almost perfectly. However, this correlation should cautiously be interpreted since the theoretical approach incorporates a number of assumptions, which might not hold true completely in practice. The results suggest that in case the mechanism II is valid, the breakdown of compressed cavities should immediately be followed by a flashover across the interface. It is, however, somewhat dubious because manifold PDIE experiments were also performed using XLPE and PEEK samples while the PD had been proven taking place at the interface. The interfaces were exposed to PD around $200\,\mathrm{pC}$ for 7 days. Fig. 5 showcases inspected aged surfaces using a digital microscope with an additional light source, where numerous cavities and a number of channels, composed of connected cavities, were observed as well as local erosion in few surfaces. It should be noted that inspected virgin surfaces did not contain such cavities or channels.

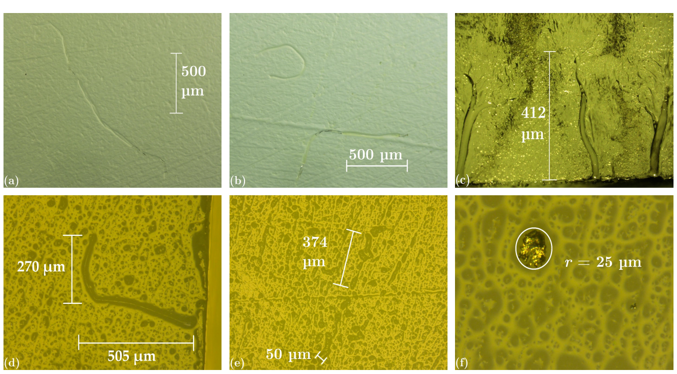

Fig. 5. First row images ($11.6\,\mathrm{bar}$): (a)-(c) Linked cavities forming long channels at the XLPE interface. Second row images ($11.6\,\mathrm{bar}$): (d) Linked cavities forming long channels at the PEEK interface. (e) Small solitary cavities (f) Erosion detected at the PEEK interface.

In the light of these observations, the following remarks are made: Since the asperities are Normally distributed [1], there are at least a few larger cavities than the estimated average cavity size. Thus, the PD activity presumably commences at the largest cavities whereas there is no activity in average-sized cavities. Hence, it is still possible that PD inception in compressed average-sized cavities evolve to a flashover instantly. Secondly, when the contact pressure is considerably increased, the cavities might become much smaller in practice than the predicted average size. Therefore, an improved model estimating the largest cavities while providing a more intricate contact analysis is likely to perform better. Thirdly, as (1) suggests, the interfacial BDS might also be influenced by the breakdown of the total area of contact, at high contact pressures in particular. The coexistence of vented cavities, enclosed cavities and large contact spots at the interface are likely to occur in real life. Depending on the contact pressure, elastic modulus and surface roughness, any of these mechanisms might predominate the rest or be equally dominant.

V. Conclusion

- The experimental results indicate that the lower the elastic modulus, the higher the BDS.
- Theoretical approaches suggest decreasing cavity size and hence the PDIE as the elastic modulus is reduced.
- As far as interfacial breakdown is concerned, the breakdown of air-filled cavities (both vented or enclosed) and the contact spots are crucially important in predominating the interfacial BDS, depending strongly on the contact pressure and elastic modulus.
- A revamped approach estimating the largest cavities while providing a more intricate contact analysis might perform better.

References

[1] E. Kantar and E. Ildstad, "Modeling longitudinal breakdown strength of solid-solid interfaces using contact theory," in *2016 IEEE Int. Conf. on Dielec. (ICD)*, vol. 1, July 2016, pp. 398–401.

[2] E. Kantar, S. Hvidsten, F. Mauseth, and E. Ildstad, "Longitudinal AC breakdown voltage of XLPE-XLPE interfaces considering surface roughness and pressure," *IEEE Trans. Dielectr. Electr. Insul.*, vol. 24, no. 5, 2017.

[3] E. Kantar, S. Hvidsten, F. Mauseth, and E. Ildstad, "On the tangential AC breakdown strength of polymeric interfaces considering elastic modulus," in *IEEE Conf. Electr. Insul. and Dielectr. Phen. (CEIDP)*, 2017.

[4] J. Greenwood and J. Williamson, "Contact of nominally flat surfaces," in *Proc. the Royal Society of London A: Mathematical, Physical and Engineering Sciences*, vol. 295, no. 1442, 1966, pp. 300–319.

[5] B. Bhushan, "Analysis of the real area of contact between a polymeric magnetic medium and a rigid surface," *Journal of Tribology*, vol. 106, no. 1, pp. 26–34, 1984.

[6] L. A. Dissado and J. C. Fothergill, *Electrical degradation and breakdown in polymers*. IET, 1992, vol. 9.

[7] E. Kantar, S. Hvidsten, F. Mauseth, and E. Ildstad, "Tangential AC breakdown strength of solid-solid interfaces considering surface roughness," in *IEEE Conf. Electr. Insul. and Dielectr. Phen. (CEIDP)*, 2017.